

# Exploring quantitative MRI contrast in posterior cortical atrophy using ex vivo imaging

Luke J. Edwards<sup>1</sup>, Carsten Jäger<sup>1</sup>, Evgeniya Kirilina<sup>1,2</sup>, Karl-Heinz Herrmann<sup>3</sup>, Kerrin J. Pine<sup>1</sup>, Patrick Scheibe<sup>1</sup>, Jürgen Reichenbach<sup>3</sup>, and Nikolaus Weiskopf<sup>1,4</sup>

<sup>1</sup> Max Planck Institute for Human Cognitive and Brain Sciences, Leipzig, Germany; <sup>2</sup> Center for Cognitive Neuroscience Berlin, Freie Universität Berlin, Berlin, Germany;

<sup>3</sup> University Clinic Jena, Jena, Germany; <sup>4</sup> Felix Bloch Institute for Solid State Physics, Leipzig University, Leipzig, Germany

ledwards@cbs.mpg.de



## Introduction

Posterior cortical atrophy (PCA) is a rare variant of Alzheimer's disease (AD) where degeneration begins in the occipital lobe rather than the hippocampus/temporal lobe [1]. Recent work has found MRI-visible breakdown of cortical lamination in AD neurodegeneration [4]. We scanned post mortem samples of PCA, AD, and control tissue with quantitative MRI metrics sensitive to cortical microstructure (R1, R2\*, mean diffusivity (MD), mean kurtosis (MK), and fractional anisotropy (FA)) [2] to investigate whether similar cortical changes occur in PCA and whether these changes qualitatively differ from those in AD. With this we aim to inform in vivo applications.

## Methods

- Formalin-fixed tissue blocks were provided by the Queen Square Brain Bank, UCL, London (QSBB); and the Brain Banking Centre Leipzig, Leipzig University (BBCL).
- Blocks scanned in 20 mm syringes in Fomblin after washing out remnant fixative with PBS.
- Multiparameter mapping data [5] recorded to map R1 and R2\* (Siemens Magnetom 7T scanner with custom CP Tx coil, 220  $\mu\text{m}$  isotropic resolution, 1.5 mm iso. B1 map).
- High resolution 50  $\mu\text{m}$  iso. T2\*w image (TE 19 ms, TR 200 ms, flip angle 50°) also recorded.
- Diffusion weighted imaging (DWI) data recorded to map MD, FA, and MK (Bruker BioSpec 94/20 9.4T preclinical scanner with cryocoil, spin echo segmented EPI DWI sequence, 200  $\mu\text{m}$  iso., 16 averages,  $b = [0.3, 2, 4, 8, 12]$  ms/ $\mu\text{m}^2$ , 60 directions each, TR 4 s, TE 25 ms).
- Cortex segmented into 20 equivolume layers based on the weighted images; as V1 images showed stria of Gennari (SoG; layer IVb) mostly in layers 8–13, parameters were binned into layers 2–7 (lower), 8–13 (mid), and 14–19 (upper).
- Tissue blocks paraffin-embedded, cut into 8  $\mu\text{m}$  sections, and processed, alternating Nissl stain and immunohistochemistry for myelin basic protein (MBP) and A $\beta$  deposits; images recorded on a Zeiss Axioscan Z1.
- Layers I–III (upper), IV (mid), and V–VI (lower) manually segmented (by CJ) on Nissl sections, projected onto the nearest MBP and A $\beta$  sections, and used to bin the average optical density.

	AD1	AD2	CTRL	PCA1	PCA2
Source	BBCL	BBCL	BBCL	QSBB	QSBB
Age/sex	81/M	77/F	49/M	75/M	71/M
PMI (hrs)	40	34	40	93	58
Regions	V1, T	V1, T	V1, T	V1, T	V1

Donor and tissue block information. PMI: post mortem interval; V1: primary visual cortex; T: temporal lobe.

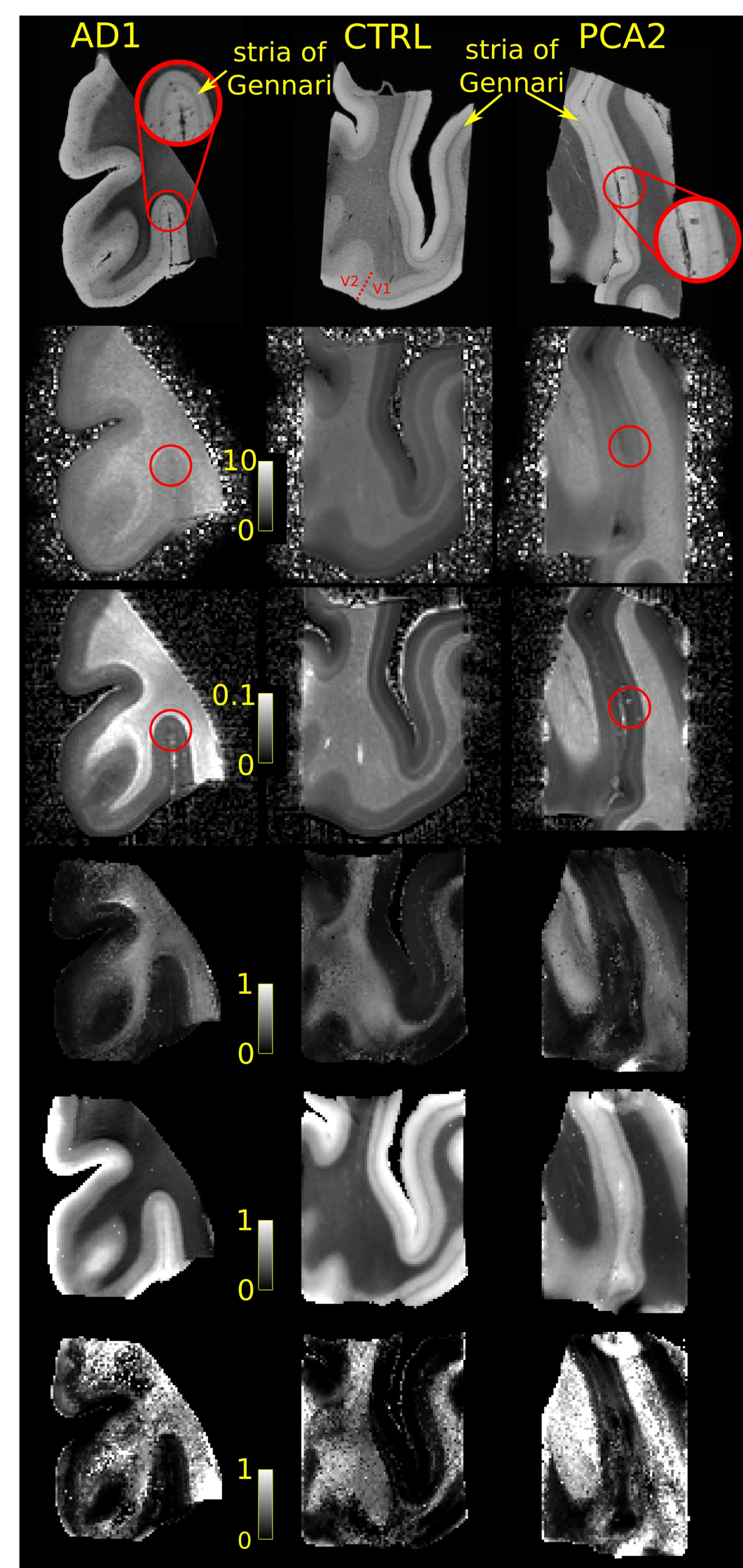
## Discussion

The quantitative MRI maps showed cortical lamination degradation relative to CTRL in MRI contrasts, in line with previous R2\* observations in post mortem AD tissue [3,4].

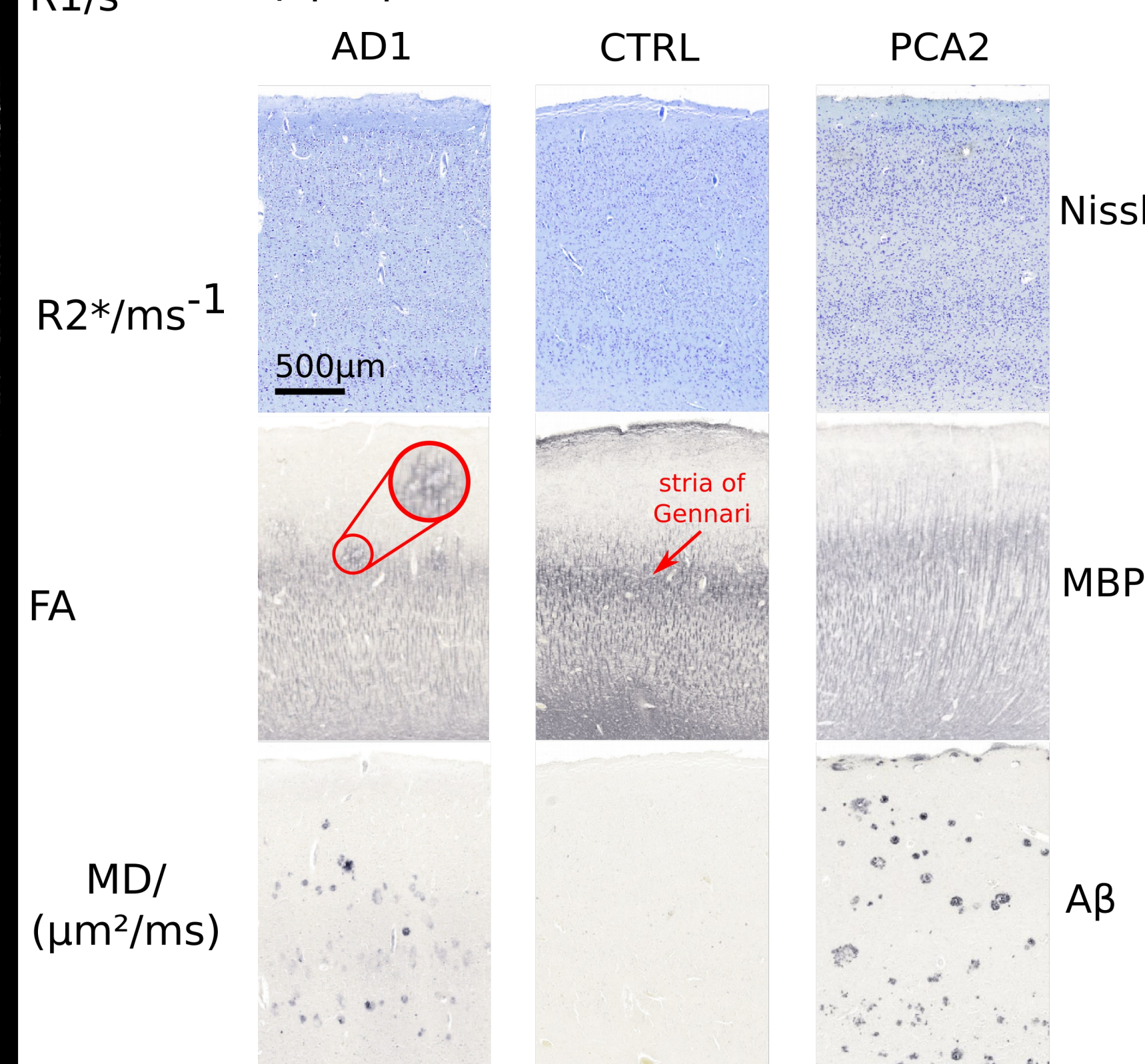
The box plots suggest that combination of regional differences in R2\*, MD, and FA profiles could potentially differentiate between AD and PCA. This differentiation could reflect differences in A $\beta$ , myelin, or iron distribution (though differences in tissue preparation cannot be completely ruled out). Quantitative iron measurements, analysis of additional samples, and in vivo experiments will allow further investigation.

We have shown that AD cortical lamination disturbances previously seen in R2\* [4] can be seen in other quantitative maps and in PCA. Observed differences in MRI contrast between PCA and AD may reflect their different progression, but the small number of samples calls for caution when extrapolating the results.

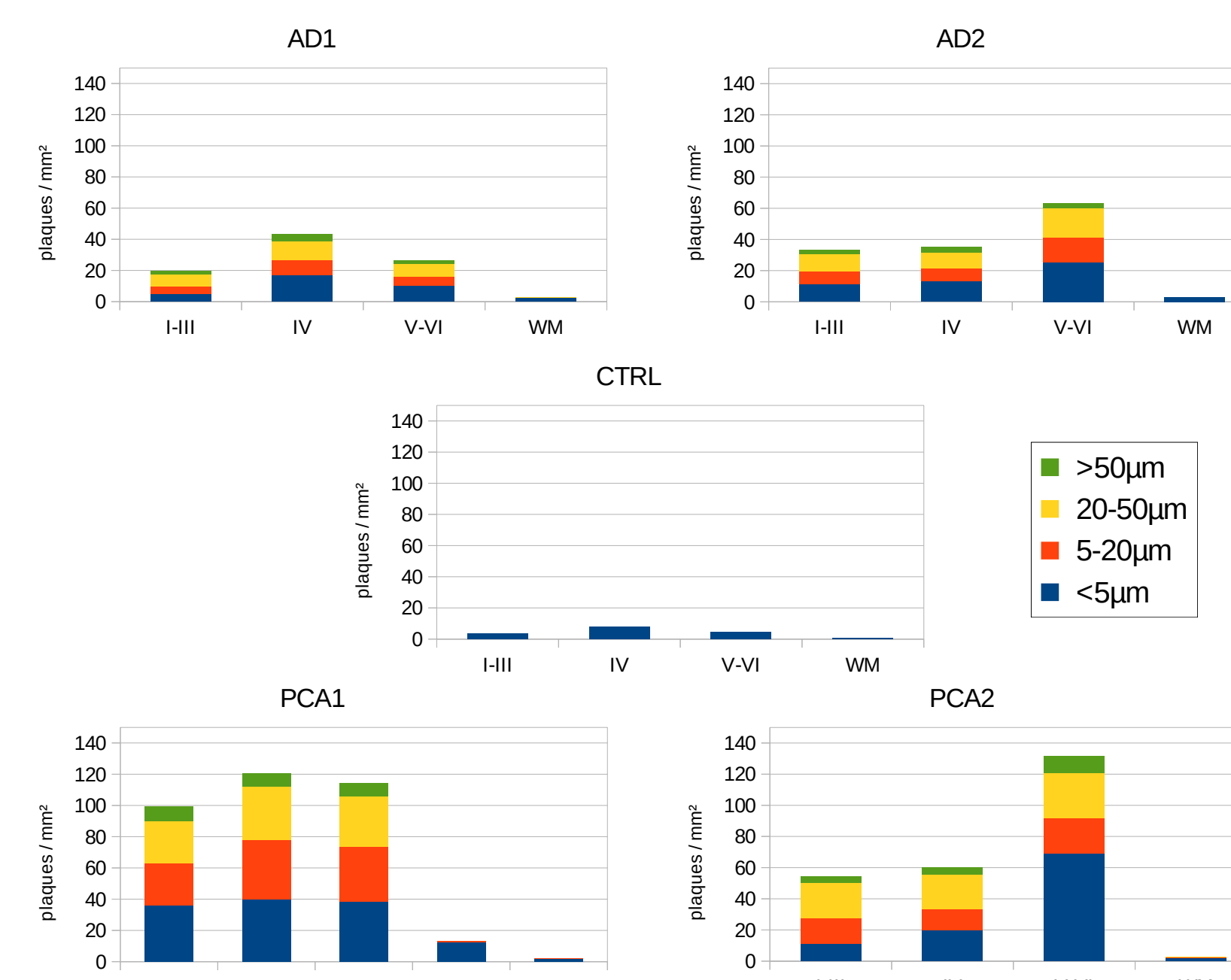
## Results



Left: Representative V1 tissue block images. In CTRL, the small region of V2 is demarked with a dashed line on the T2\*w image. Compared to CTRL, PCA and AD samples show a much less distinct SoG in R1 and R2\*, in line with laminar breakdown in post mortem AD tissue [3,4]. T2\*w images suggest localisation of some laminar degradation with clusters of hypointensities (circles); these could relate to A $\beta$  plaques.

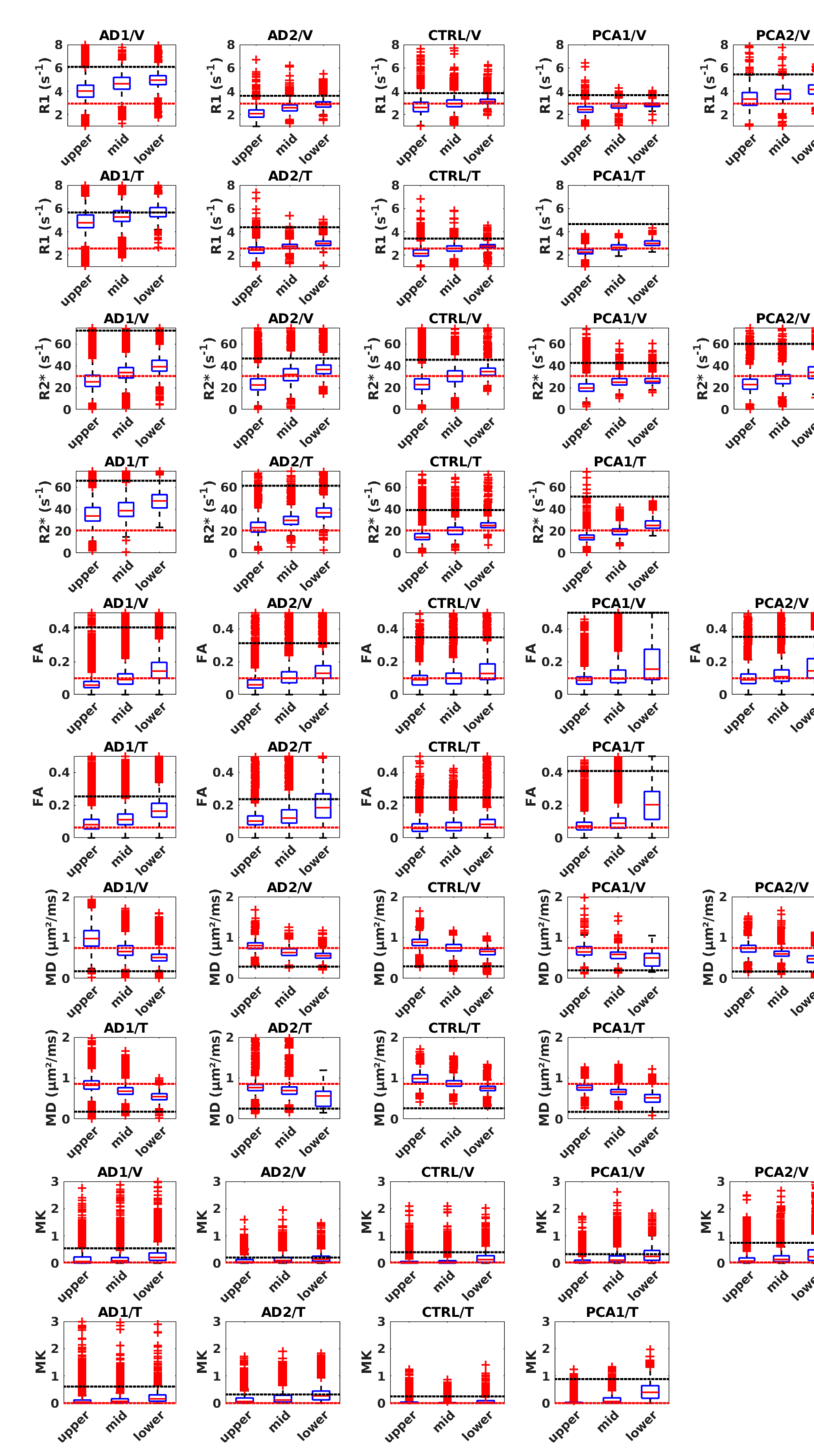
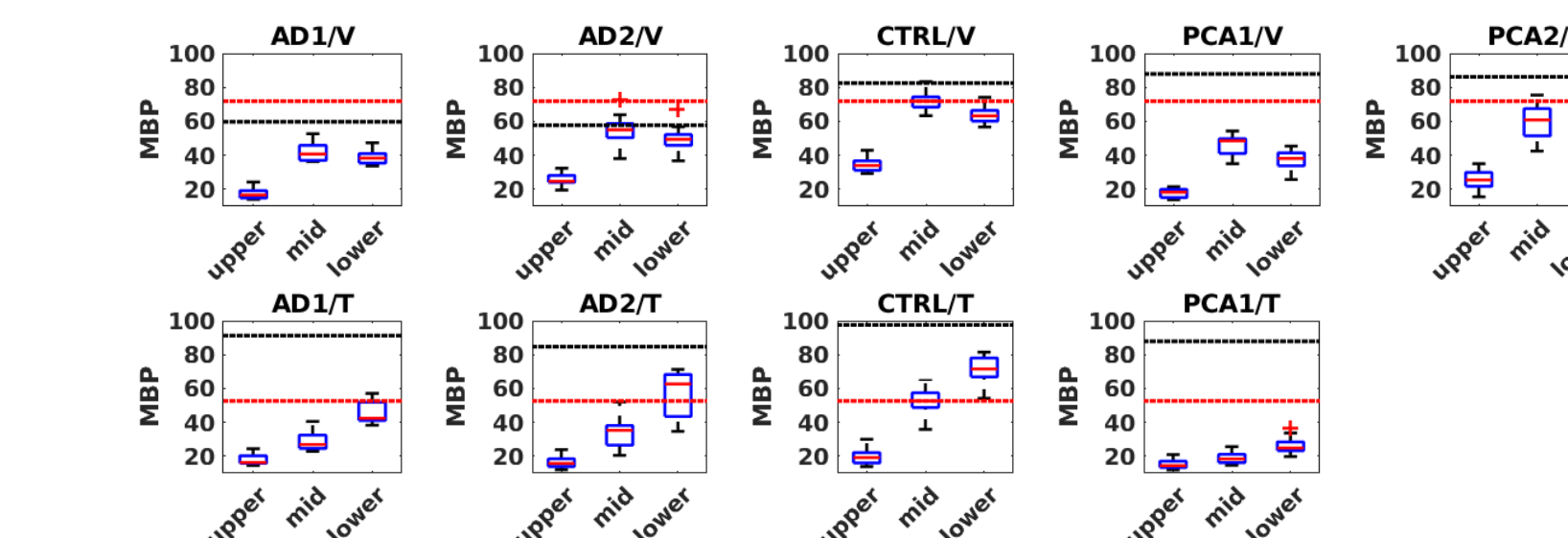


Above: Histological sections taken from V1. A $\beta$  plaques evident in AD and PCA, but not in CTRL. PCA plaques more diffuse than AD. SoG only well-defined in CTRL MBP stain (arrow). Spherical myelin disturbances seen in AD (circle) were found to relate to A $\beta$  plaques.



Above: Quantitative A $\beta$  plaque counts categorised per diameter, calculated per 1 mm<sup>2</sup> in V1 samples. CTRL only shows small A $\beta$  deposits, rather than pathological plaques. Laminar differences can be seen between AD cases and PCA cases, potentially representing different subtypes. Number of plaques higher in PCA, in line with pathological development starting in the occipital lobe.

Below and right: Laminar distributions of MRI and histological parameters. Box: median and 25 and 75% percentiles; whiskers: most extreme value (excluding outliers); crosses: outliers; black dashed line: median white matter value; dashed red line: median mid-CTRL value. Differential effects in the AD and PCA samples relative to CTRL imply combination of maps could potentially distinguish AD and PCA.



## Acknowledgements

The research leading to these results has received funding from the European Research Council under the European Union's Seventh Framework Programme (FP7/2007-2013) / ERC grant agreement no. 616905.



## References

- Crutch, SJ et al. (2016), Current Directions in Psychological Science, doi:10.1177/0963721416655999
- Edwards, LJ et al. (2018), Microstructural imaging of human neocortex in vivo, Neuroimage, doi:10.1016/j.neuroimage.2018.02.055
- Kenkuis, B et al. (2019), Neuroimage Clinical, doi:10.1016/j.nicl.2019.101665
- Nabuurs, RJA et al. (2013), Journal of Alzheimer's Disease, doi:10.3233/JAD-122215
- Weiskopf, N et al. (2013), Front. Neurosci., doi:10.3389/fnins.2013.00095